

Beta-trees: Multivariate histograms with confidence statements

Guenther Walther^{1*} and Qian Zhao²

¹Department of Statistics and ²Department of Biomedical Data Science
Stanford University

{gwalth, qzhao1}@stanford.edu

July 2023

Abstract

Multivariate histograms are difficult to construct due to the curse of dimensionality. Motivated by k -d trees in computer science, we show how to construct an efficient data-adaptive partition of Euclidean space that possesses the following two properties: With high confidence the distribution from which the data are generated is close to uniform on each rectangle of the partition; and despite the data-dependent construction we can give guaranteed finite sample simultaneous confidence intervals for the probabilities (and hence for the average densities) of each rectangle in the partition. This partition will automatically adapt to the sizes of the regions where the distribution is close to uniform. The methodology produces confidence intervals whose widths depend only on the probability content of the rectangles and not on the dimensionality of the space, thus avoiding the curse of dimensionality. Moreover, the widths essentially match the optimal widths in the univariate setting. The simultaneous validity of the confidence intervals allows to use this construction, which we call *Beta-trees*, for various data-analytic purposes. We illustrate this by using Beta-trees for visualizing data and for multivariate mode-hunting.

1 Introduction

This paper is concerned with constructing multivariate data summaries for inference. The classical example of such a data summary is the histogram, which approximates a distribution with a distribution that is piecewise uniform over rectangles. The two main purposes of a histogram are to approximate the probability content of subregions and, especially in a lower dimensional setting, to visualize the data. Another important purpose of the histogram is statistical inference. A relevant example, which is addressed in some detail in Section 6, is the analysis of flow cytometry data. Such data represent multiple parameters of a single cell and an important task in the analysis of such data is to detect and isolate subpopulations of cells. One standard approach to this problem is to construct a multivariate histogram or density estimate and to identify subpopulations with high density regions [32]. However, such a density estimate does not provide any confidence statement about the presence of high density regions separated by a region of low density. It is a notoriously difficult problem to construct density estimates in a multivariate setting due to the ‘curse of dimensionality’; this problem is compounded by the need to find corresponding standard errors and to adjust for data snooping when searching for high density regions. In fact, while the vast amount of flow cytometry data which has become available

*Research supported by NSF grant DMS-1916074

via modern high-throughput instrumentation has spurred the development of a large number of algorithms to automate this analysis [51, 3, 7, 36], those algorithms generally do not provide any confidence statements about their findings, and there is a widely recognized need for a principled analysis based on statistical guarantees [7, 31, 12].

Section 6 shows how the methodology introduced in this paper can be applied to the cytometry problem to provide guaranteed finite-sample confidence bounds that allow the detection of such high density regions. A key point is that the widths of these confidence intervals depend essentially only on the probability content of the region under consideration and not on the dimensionality of the space, thus avoiding the curse of dimensionality. Developing such statistical methodology is crucial for the quest of the flow cytometry community to discover biological insights by increasing the dimension of the measurements without having to incur a large penalty in power compared to performing statistical analyses in a lower dimensional space.

Another example where multivariate density estimates are being used extensively is in databases, where histograms constitute the most common tool for the succinct approximation of data [24, 47, 20, 23, 1]. This is motivated by the fact that often a dataset cannot be stored in its entirety, so it is necessary to construct a summary (synopsis). Databases typically summarize data by means of a histogram, and the summary is then used to answer various types of queries in the same way the original data would have been used [24]. Since such a summary of data via a histogram will result in some loss of information, it is critically important to provide error bounds (‘quality guarantees’) for these histogram estimates. This has led to a recent active research effort in the computer science community to derive quality guarantees for histograms [1, 2, 11, 14, 13, 47]. The methodology developed here can be evolved to produce better quality guarantees in that context, and we will report on this aspect in a different paper.

There are a number of other areas where multivariate histograms play an increasingly important role, most notably in astronomy and particle physics, see [37, 40, 35] for surveys. While there has been an intensive effort in the statistical research community during the last 40 years to develop increasingly sophisticated density estimation methods, the histogram continues to be surprisingly popular. The following statement from the astronomical overview paper [40] is illuminating as to why the histogram is a preferred tool in modern astronomical research:

”For example, while smoothed plots of pulses within gamma-ray bursts (GRBs) make pretty pictures, one is really interested in pulse locations, lags,... All of these quantities can be determined directly from the locations, heights, and widths of the blocks [of the histogram] - accurately and free of any smoothness assumptions.”

Implicit in this statement is the claim that an appropriately constructed histogram gives a simple summary of the data (in terms of a piecewise constant function) while still allowing to infer the relevant features of the data. Of course, the key point here is that the histogram needs to be constructed appropriately, i.e. by choosing the partition (the number and location of the bins) appropriately. The definition of the histogram does not specify these parameters and leaves that choice to the data analyst [17]. The main contribution of this paper is to provide such a specification which results in favorable statistical properties. Our method is motivated by k -d trees in computer science, which produce an efficient partition of space that adapts to the data. It turns out that important statistical properties of such k -d trees can be described by the beta distribution. We then show how this fact can be used to prune the k -d tree in a data-adaptive way such the resulting partition has the following two properties: First, with high confidence the distribution is close to uniform on each rectangle of the partition. Second, despite the data-dependent construction we can give guaranteed finite sample simultaneous confidence bounds for the probabilities (and hence for the average densities) of each rectangle in the partition. These two properties show

that the resulting histogram is an appropriate summary of multivariate data that allows finite sample inference for the tasks described above. Moreover, using the multi-scale Bonferroni adjustment of [50] results in widths of these confidence intervals that do not depend on the dimension of the space, and furthermore the widths match the optimal widths in a univariate setting. In that sense the methodology avoids the curse of dimensionality.

k -d trees are a popular data structure in computer science that is effective for several important applications involving multivariate data. In contrast, its statistical properties in terms of the beta distribution do not yet seem to be available in the literature about k -d trees. These statistical properties together with the multi-scale Bonferroni adjustment of [50] are the key components for the proposed methodology, which we therefore call *Beta-tree*.

Before describing our method in Section 2, we give a review of prior work that is relevant for the problem considered here. In the univariate setting, [16] and [6] derive rules for choosing the number of bins in a histogram when the bin widths are of equal size. The common approach is to regard the histogram as a density estimator and to minimize the asymptotic mean integrated square error, which is of order $n^{-2/3}$. In contrast, in the d -dimensional setting this optimal error is of the order $O(n^{-\frac{2}{2+d}})$, [41, Section 3.4]. Analogous results obtain when employing other standard density estimators, such as the kernel density estimator, see [45]. These results show that in order to achieve the same mean integrated square error as in the univariate case, the number of observations needs to increase *exponentially* with the dimension d . This phenomenon is known as the curse of dimensionality. While the name was introduced by [4] in connection with computational effort, the statistical version of the curse of dimensionality refers to the phenomenon that data become sparse in high dimensional space. For instance, if one samples n observations from a uniform distribution in a d -dimensional unit cube, then the number of points in a sub-cube with side length r is about nr^d . Hence in order to obtain the same number of observations in the sub-cube as in the univariate case, the number of observations needs to increase exponentially with the dimension d .

There are several proposals in the literature that involve an adaptive partition of multivariate space, see [34, 25, 37, 30, 28, 29, 26]. These proposals use a penalty criterion or maximum likelihood in order to select a partition out of a collection of candidate partitions, where the candidate partitions are obtained from a starting rectangle by recursively subdividing according to Lebesgue measure. The main statistical results of these papers are rates of convergence for the density estimator resulting from the adaptive partition. For example, [28] show that when the underlying density can be approximated well by functions that are piecewise constant on a dyadic partition, then the rate of convergence does not depend on the dimension of the space. However, none of these proposals provide statistical guarantees such as confidence bounds, which are required for statistical inference such as the mode-hunting problem addressed below. A key distinction in our construction is that the recursive partitioning is done according to empirical measure rather than Lebesgue measure. This allows to obtain finite sample confidence bounds for the probability content of the resulting rectangles despite the fact that the construction was performed in a data-dependent way.

1.1 Contributions of his paper

The prior methods reviewed above assess histogram accuracy in terms of *aggregated* accuracy over the entire space, such as Hellinger distance and KL-divergence. The resulting rates of convergence do not provide any statistical guarantees such as confidence bounds. In this paper, we consider the original purpose of the histogram: providing good simultaneous estimates for probabilities over rectangles. We construct a concise summary of multivariate data in terms of a histogram such that with high confidence the distribution is close to uniform on each rectangle in the partition. We obtain simultaneous confidence intervals for the probabilities of these rectangles that satisfy finite sample guarantees. We also show that the lengths of these confidence intervals are

close to the optimal lengths in the univariate setting, so this method pays only a very small price for analyzing multivariate data and therefore avoids the curse of dimensionality. These theoretical results are derived assuming only that the distribution is continuous.

The Beta-tree histogram can be seen as the statistical counterpart of the k -d tree, and it shares the advantageous property of a compact representation of the data. The Beta-tree prunes subtrees of the k -d tree such that the resulting histogram has fewer regions in the partition while still passing an appropriate goodness-of-fit test. As in the case of the k -d tree, the computational complexity of the Beta-tree is essentially linear in the sample size, irrespective of the dimension.

Our approach is motivated by the essential histogram of [27], which is the univariate histogram with the fewest number of bins that still passes the generalized likelihood ratio test. The essential histogram also provides statistical guarantees, but it is not clear how to extend the essential histogram to the multivariate setting. The key difficulty is to construct an adaptive partition; furthermore, it is not clear how to carry out the likelihood ratio test on such a data-adaptive partition. The Beta-tree addresses the first problem by pruning subtrees of the k -d tree rather than adding splits to the partition based on an optimization problem. It addresses the second problem by applying the multiscale Bonferroni adjustment of [50] to the resulting exact beta distributions rather than applying a scale-dependent penalty on the likelihood ratio statistic. The Beta-tree may therefore have some superfluous splits, but we submit that there is not much gained by insisting on the minimum number of splits. In turn, the Beta-tree is much faster to compute than the univariate essential histogram and moreover appears to produce tighter confidence bounds in the univariate setting.

In the remainder of this article, we will describe our method in Section 2 and illustrate our method for data visualization in Section 4, for mode hunting in Section 5, and with a real data example in Section 6. In particular, Section 5 shows how the simultaneous inference may be used for multivariate cluster analysis, which may be of independent interest. Proofs are deferred to Section 8.

2 Constructing the Beta-tree

The construction of the Beta-tree proceeds as follows: We grow a k -d tree and then on each node (i.e. rectangle) that is bounded, we perform a goodness-of-fit test to decide whether the data on that rectangle follow a uniform distribution; if so, we cut the sub-tree below that rectangle.

The goodness-of-fit test checks uniformity on a rectangle R by examining the empirical density on the sub-rectangles of R in the k -d tree. This analysis requires to construct simultaneous confidence intervals for the probability contents of all rectangles in the k -d tree. It turns out that it is possible to derive such confidence intervals with an exact finite sample level, despite the data-adaptive nature of the k -d tree. Moreover, by applying a certain weighted multiscale Bonferroni adjustment, it is possible to construct the simultaneous confidence intervals such that their widths match the optimal univariate widths.

The details for these various items are given in the following subsections.

2.1 Building a space partition with a k -d tree

Given d -dimensional data $X_i = (X_{i1}, \dots, X_{id})$, $i = 1, \dots, n$, we apply the following recursive space-partitioning scheme. Apart from some details, this amounts to building a k -d tree, see [5, 19]:

We split $R_0 := \mathbf{R}^d$ into two halfspaces by cutting the p th coordinate (starting with $p = 1$) at an order statistic

of $\{X_{ip}, i = 1, \dots, n\}$ such that (about) half of the observations fall in each of the resulting two halfspaces:

$$R_1 := \{x \in R_0 : x_p < X_{(\lfloor \frac{n}{2} \rfloor), p}\}, \quad R_2 := \{x \in R_0 : x_p > X_{(\lfloor \frac{n}{2} \rfloor), p}\}.$$

Then we recursively apply this partitioning scheme in R_1 , using only the observations that fall into R_1 when computing the median, and likewise for R_2 . Thus the rectangle R_k is split into two children rectangles R_{2k+1} and R_{2k+2} at a marginal median of the data in R_k . Note that the observations that determine the boundaries do not belong to any R_k . We let p cycle through $\{1, \dots, d\}$ as we progress through the recursion. That is, we set $p = D \bmod d + 1$, where $D = \lfloor \log_2(k + 1) \rfloor$ is the tree depth of R_k . We stop splitting R_k once it has fewer than $4 \log n$ observations.

Some rectangles R_k in the k -d tree will be unbounded, whereas the construction of a histogram is necessarily restricted to bounded rectangles. The following modification produces a k -d tree with only bounded rectangles, which allows to extend the construction of a histogram further out into the tails of the data: We create a bounding box by discarding the observations with the smallest and with the largest order statistic in the first coordinate, and we use these two order statistics (or some other order statistics if one wishes to cut a larger fraction of the observations) as bounding values in the first coordinate. We iterate this process through all d coordinates. Then we run the above space-partitioning algorithm on the remaining observations with R_0 equaling the bounding box. Importantly, all of the statistical methodology described below continues to hold with this modification, in particular the crucial finite sample result given in Proposition 1.

If the data X_{1p}, \dots, X_{np} are distinct for each coordinate p , then the number of observations n_k in R_k is a function of n and k only. It is convenient to define the empirical measure as $F_n(R_k) = \frac{n_k + 1}{n}$ rather than $\frac{n_k}{n}$. We discuss this as well as other relevant aspects of k -d trees in Appendix A.

2.2 Deriving exact confidence bounds for the rectangles in the k -d tree

We denote the distribution of the X_i by F . The following proposition is the starting point for our construction. It shows that $F(R_k)$ follows a beta distribution whose parameters depend only on n_k and the sample size n :

Proposition 1 *Let $X_i, i = 1, \dots, n$, be i.i.d. F , where F is a continuous distribution on \mathbf{R}^d . Then every rectangle R_k generated by the partitioning scheme in Section 2.1 is a random set containing a deterministic number n_k of observations in its interior and the random variable $F(R_k)$ satisfies*

$$F(R_k) \sim \text{Beta}(n_k + 1, n - n_k).$$

This result is related to early results by Wald (1943) and Tukey (1947), see the comments in the proof in Section 8. We note that Proposition 1 remains valid for other ways of choosing the axis p for the split, e.g. choosing p randomly, as well as for other ways to set n_k , as long as these do not depend on the data $\{X_i\}_{i=1}^n$.

An important consequence of Proposition 1 is that $F(R_k)$ is a pivotal quantity, i.e. its distribution does not depend of F . Furthermore, this distribution is known exactly. This is a multivariate generalization of the well known fact that in the univariate case $F((X_{(i)}, X_{(j)})) \sim \text{Beta}(j - i, n + 1 - (j - i))$, see Shorack and Wellner (1986) [43, Chapter 3.1]. We note that this property depends crucially on employing the data adaptive collection $\{R_k\}$ rather than constructing a partition by splitting according to Euclidean distance as is usually done in the literature.

Proposition 1 implies an exact $(1 - \alpha)$ level confidence interval for $F(R_k)$:

$$C_k(\alpha) := \left(q\text{Beta}\left(\frac{\alpha}{2}, n_k + 1, n - n_k\right), q\text{Beta}\left(1 - \frac{\alpha}{2}, n_k + 1, n - n_k\right) \right) \quad (1)$$

where $q\text{Beta}(\alpha, \cdot, \cdot)$ denotes the α -quantile of the beta distribution with the given degrees of freedom. Strictly speaking, this is a prediction interval or a tolerance region since $F(R_k)$ is a random variable, which measures the probability content of the random set R_k . Likewise, an exact $(1 - \alpha)$ level confidence interval for the average density $f(R_k) = F(R_k)/|R_k|$ is given by dividing the bounds in (1) by the volume $|R_k|$, see (3) below.

2.3 Constructing simultaneous confidence bounds with a multiscale Bonferroni adjustment

In order to construct confidence intervals for the $F(R_k)$ and $f(R_k) = F(R_k)/|R_k|$ that are simultaneously valid for all rectangles R_k in the k -d tree, we use the weighted Bonferroni adjustment that [50] propose for univariate scan statistics. The motivation for using that weighted adjustment is to obtain good statistical performance across all scales, which in this context means across all tree depths D . The prescription given in [50] is to assign the same significance level to each interval at a given scale, and to weigh the significance level across scales according to a harmonic sequence so that the smallest scale is weighted with a factor $\frac{1}{2}$, the second smallest scale with a factor $\frac{1}{3}$ etc. Translated to the setting of a k -d tree with R_0 being a bounding box, this prescription assigns each of the N_D bounded rectangles at tree depth D the significance level

$$\alpha_D = \frac{\alpha}{N_D(D_{max} - D + 2) \sum_{B=2}^{D_{max}+1} \frac{1}{B}}, \quad D \geq 1, \quad (2)$$

where D_{max} is the maximum depth of the Beta-tree, and $\alpha_0 = 0$. Therefore, if R_k has tree depth D , then

$$\text{lower}(R_k) = \frac{q\text{Beta}\left(\frac{\alpha_D}{2}, n_k + 1, n - n_k\right)}{|R_k|}, \quad \text{upper}(R_k) = \frac{q\text{Beta}\left(1 - \frac{\alpha_D}{2}, n_k + 1, n - n_k\right)}{|R_k|}, \quad (3)$$

provide lower and upper confidence bounds for $f(R_k) = F(R_k)/|R_k|$, and these confidence bounds have simultaneous coverage level $1 - \alpha$ for all bounded R_k since the corresponding α_D sum to α .

Likewise, using $C_k(\alpha_D)$ in (1) gives simultaneous confidence bounds for the $F(R_k)$.

If R_0 equals \mathbf{R}^d rather than a bounding box, then there will be no bounded rectangles at the smallest depths D and (2) changes accordingly. Appendix A gives the details.

2.4 Pruning the k -d tree by checking goodness-of-fit

A key principle for constructing a histogram is to find a parsimonious representation which still gives an good approximation to the distribution, see e.g. the discussion in [27]. This principle can be readily implemented for a nested partition as follows: We keep the largest rectangles R_k for which we are confident that the distribution of the data on R_k is the uniform distribution specified by a histogram that uses R_k as a bin¹. Assessing whether the distribution is uniform on a rectangle R_k amounts to a goodness-of-fit test. Such a test can be readily implemented for the multiscale partition given by the k -d tree since the rectangles $R \subset R_k$ constitute an appropriate collection of test sets for which we can compare the empirical density to that on R_k . This simply amounts to checking whether the empirical density on R_k lies in all the confidence intervals (3) for the $f(R)$, $R \subset R_k$, i.e.

¹More precisely, the GOF test is not about the conditional distribution on R_k but about the unconditional F restricted to R_k

in the intersection of these confidence intervals. This intersection is given by $(\widetilde{\text{lower}}(R_k), \widetilde{\text{upper}}(R_k))$, where these bounds are defined recursively as follows:

$$\begin{aligned}\widetilde{\text{lower}}(R_k) &= \max\left(\text{lower}(R_k), \widetilde{\text{lower}}(\text{1st child of } R_k), \widetilde{\text{lower}}(\text{2nd child of } R_k)\right) \\ \widetilde{\text{upper}}(R_k) &= \min\left(\text{upper}(R_k), \widetilde{\text{upper}}(\text{1st child of } R_k), \widetilde{\text{upper}}(\text{2nd child of } R_k)\right)\end{aligned}\quad (4)$$

if R_k has children, otherwise $\widetilde{\text{lower}}(R_k) = \text{lower}(R_k)$ and $\widetilde{\text{upper}}(R_k) = \text{upper}(R_k)$.

Now we can define the *Beta-tree* as the collection of the maximal (with respect to inclusion) bounded rectangles of the k -d tree that pass the goodness-of-fit test. That is, we take all rectangles R_k that are bounded and satisfy $\widetilde{\text{lower}}(R_k) \leq h_k \leq \widetilde{\text{upper}}(R_k)$ while none of the ancestors of R_k satisfy these two conditions. Here h_k is the empirical average density of R_k :

$$h_k := \frac{F_n(R_k)}{|R_k|} = \frac{n_k + 1}{n|R_k|}\quad (5)$$

The tree structure makes it easy to find these maximal rectangles recursively or iteratively, see Appendix A.

The *Beta-tree histogram* is the histogram constructed using the rectangles in the Beta-tree. That is, on the rectangle R_k the histogram has height h_k given by (5). The Beta-tree histogram lies in the $(1 - \alpha)$ confidence set for F that is given by the multiscale goodness-of-fit test, and it is the most parsimonious distribution in that confidence set among histograms that use rectangles in the k -d tree as potential bins.

3 The simultaneous confidence intervals attain the optimal univariate widths

The Beta-tree satisfies a key goal of the histogram: It provides a parsimonious summary of the data while still giving a good approximation to the distribution. Importantly, the data-adaptive construction using the goodness-of-fit test described in the previous section does not invalidate the statistical guarantees (3) for $f(R_k)$, since those confidence bounds are simultaneous for all R_k . This raises the question whether this simultaneity results in overly conservative confidence bounds. It turns out that this is not the case: In fact, the widths of the confidence intervals essentially match the optimal simultaneous widths in the *univariate* setting. This shows that this data-adaptive construction avoids the curse of dimensionality, and there is only an asymptotically negligible price to pay compared to the univariate setting for effectively summarizing multivariate data with a histogram.

To make this precise, we first summarize the relevant lower bound in the univariate case. It is well known that the empirical measure of an interval I , $F_n(I)$, estimates $F(I)$ with precision $\sqrt{n} \frac{|F_n(I) - F(I)|}{\sqrt{F(I)(1-F(I))}} = O_p(1)$.

If one wishes to estimate $F(I)$ simultaneously for all intervals I , then there is an unavoidable penalty of size $\sqrt{2 \log \frac{e}{F(I)}}$: Theorem 1 in [27] shows that if $\mathcal{J}_n = \bigcup_i I_{i,n}$ is a partition of the line such that $F(I_{i,n}) = p_n$, $i = 1, \dots, \lfloor \frac{1}{p_n} \rfloor$ and $\frac{\log^2 n}{n} \leq p_n \rightarrow 0$, then

$$\mathbb{P}_F\left(\text{for some } I \in \mathcal{J}_n : \sqrt{n} \frac{|F(I) - F_n(I)|}{\sqrt{F(I)(1-F(I))}} \geq (\sqrt{2} - \epsilon_n) \sqrt{\log \frac{e}{F(I)}}\right) \rightarrow 1 \quad (n \rightarrow \infty) \quad (6)$$

with $\epsilon_n \rightarrow 0$ at a certain rate. Moreover, this penalty cannot be improved with any other estimator in place of F_n . The constant $\sqrt{2}$ is important as it measures the difficulty of the estimation problem, see [50]. The lower

bound (6) implies a lower bound for any confidence interval C for $F(I)$, because if $|F(I) - F_n(I)|$ satisfies a lower bound, then the radius $\sup_{G \in C} |G - F_n(I)|$ must also satisfy this bound.

Theorem 1 shows that despite the data-adaptive construction in multivariate space, the simultaneous confidence intervals $C_k(\alpha_D)$ attain the critical constant $\sqrt{2}$ of the univariate lower bound (6), up to a term $\epsilon_n \rightarrow 0$:

Theorem 1 *If F is a continuous distribution on \mathbf{R}^d , then for every k with $n_k \in [\log^2 n, n^q]$, $q \in (0, 1)$, the confidence interval $C_k(\alpha_D)$ for $F(R_k)$ satisfies*

$$\sup_{G \in C_k(\alpha_D)} \sqrt{n} \frac{|G - F_n(R_k)|}{\sqrt{G(1-G)}} \leq \left(\sqrt{2} + \frac{4}{\sqrt{\log n}} \right) \sqrt{\log \frac{e}{G}}$$

Some remarks:

1. Note that the theorem applies to all confidence intervals in the k -d tree, not just those of the pruned Beta-tree.

2. The inequality in the theorem is deterministic: While R_k is random, $F_n(R_k) = \frac{n_k+1}{n}$ as well as $C_k(\alpha)$ are deterministic. In particular, the above inequality holds uniformly in k .

3. The theorem applies to rectangles R_k that are not very large, i.e. $n_k \leq n^q$. A different Bonferroni weighting would allow to extend the theorem to all rectangle sizes, but the discussion in [50] for the univariate regression setting suggests that it is worthwhile to trade off the optimality for large rectangles in order to obtain a better finite sample performance for smaller rectangles, which are typically more relevant in practice.

4 Summarizing data using the Beta-tree histogram

In this section we apply the Beta-tree histogram to summarize two- and three- dimensional data from various distributions. The left plot in Figure 1 shows the Beta-tree for a sample from a two-dimensional normal distribution with correlation coefficient 0.5, while right plot shows the Beta-tree with a bounding box for a bivariate uniform distribution. Both samples have sizes $n = 1000$ and the bounding box is constructed as described in Section 2.1 by excluding 0.5% of the data in each tail of each coordinate.

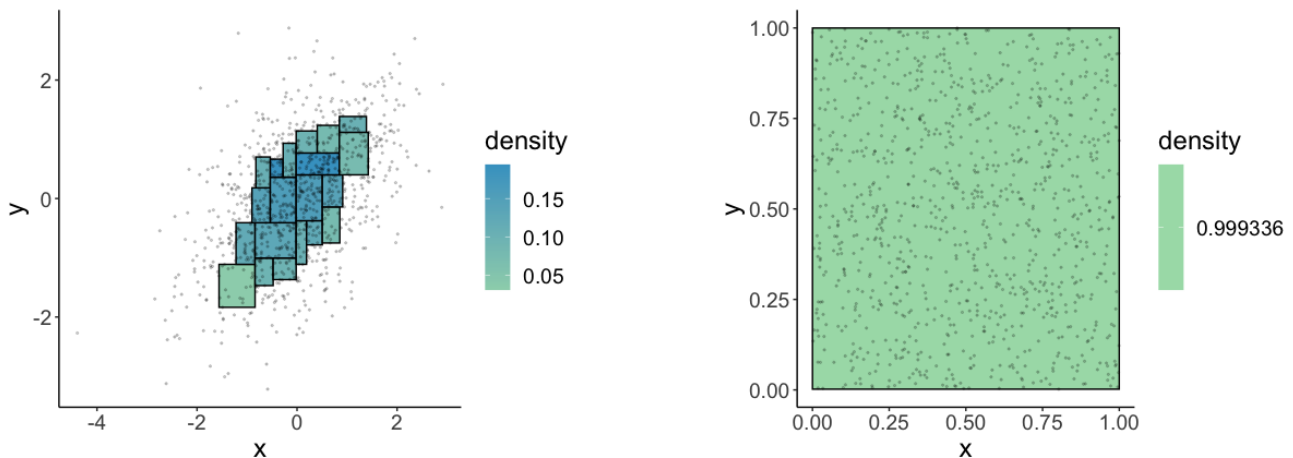


Figure 1: Beta-tree histograms for samples from a bivariate normal (left) and a bivariate uniform (right), $n = 1000$.

Figure 2 shows the Beta-tree histogram with and without bounding box for a larger sample of size $n = 20000$ from the same bivariate normal distribution. Due to the construction via the multiscale goodness-of-fit test, the Beta-tree histogram produces larger bins where the density does not change much and smaller bins where the density changes quickly. This is an important and necessary feature in order to obtain a summary that is both parsimonious and accurate. In particular, the uniform distribution in Figure 1 results in a single bin for the Beta-tree. This desirable outcome is notoriously difficult to achieve with other histogram rules.

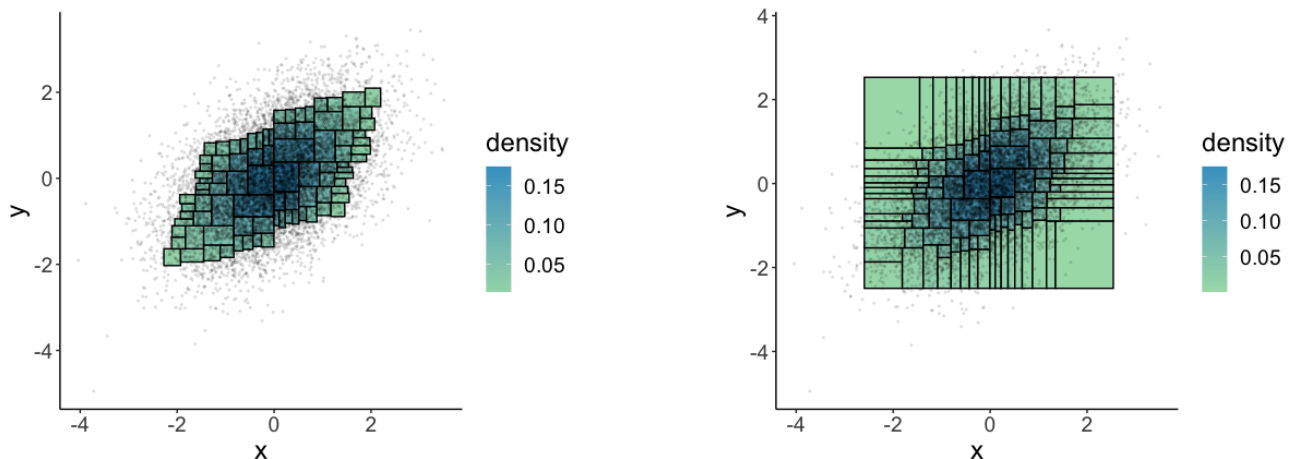


Figure 2: Beta-tree histograms without a bounding box (left) and with a bounding box (right), $n = 20000$.

In order to evaluate the Beta-tree for more complex distributions we consider two- and three- dimensional data from mixtures of multivariate Gaussian distributions. We consider the following two scenarios:

In the first scenario, we sample $n = 2000$ observations from the following two-dimensional mixture:

$$\frac{2}{5}\mathcal{N}\left(\begin{pmatrix} -1.5 \\ 0.6 \end{pmatrix}, \begin{pmatrix} 1 & 0.5 \\ 0.5 & 1 \end{pmatrix}\right) + \frac{3}{5}\mathcal{N}\left(\begin{pmatrix} 2 \\ -1.5 \end{pmatrix}, \begin{pmatrix} 1 & 0 \\ 0 & 1 \end{pmatrix}\right).$$

In the second scenario, we sample $n = 20,000$ observations from the three-dimensional mixture

$$\begin{aligned} \frac{2}{5}\mathcal{N}\left(\begin{pmatrix} -1.5 \\ 0.6 \\ 1 \end{pmatrix}, \begin{pmatrix} 1 & 0.5 & 0.5 \\ 0.5 & 1 & 0.5 \\ 0.5 & 0.5 & 1 \end{pmatrix}\right) + \frac{2}{5}\mathcal{N}\left(\begin{pmatrix} 2 \\ -1.5 \\ 0 \end{pmatrix}, \begin{pmatrix} 1 & 0 & 0 \\ 0 & 1 & 0 \\ 0 & 0 & 1 \end{pmatrix}\right) \\ + \frac{1}{5}\mathcal{N}\left(\begin{pmatrix} -2.6 \\ -3 \\ -2 \end{pmatrix}, \begin{pmatrix} 1 & -0.4 & 0.6 \\ -0.4 & 1 & 0 \\ 0.6 & 0 & 1 \end{pmatrix}\right). \end{aligned}$$

We chose these two distributions because some of the components are correlated and because individual components are relatively disjoint from each other. For example, if we were to classify which component an observation is sampled from using a Bayes classifier, then the accuracy is over 98% in both scenarios.

We compare three ways to visualize the data. First, we use a kernel density estimate. In more detail, we use a Gaussian kernel and select the bandwidth with biased cross-validation [39] in two dimensions and with the plug-in bandwidth estimator [42, 52, 10] in three dimensions. Both estimates are implemented in the R package `ks`. The kernel density estimates are shown in Figures 3a and 4a. In Figure 4 we plot the estimated density along

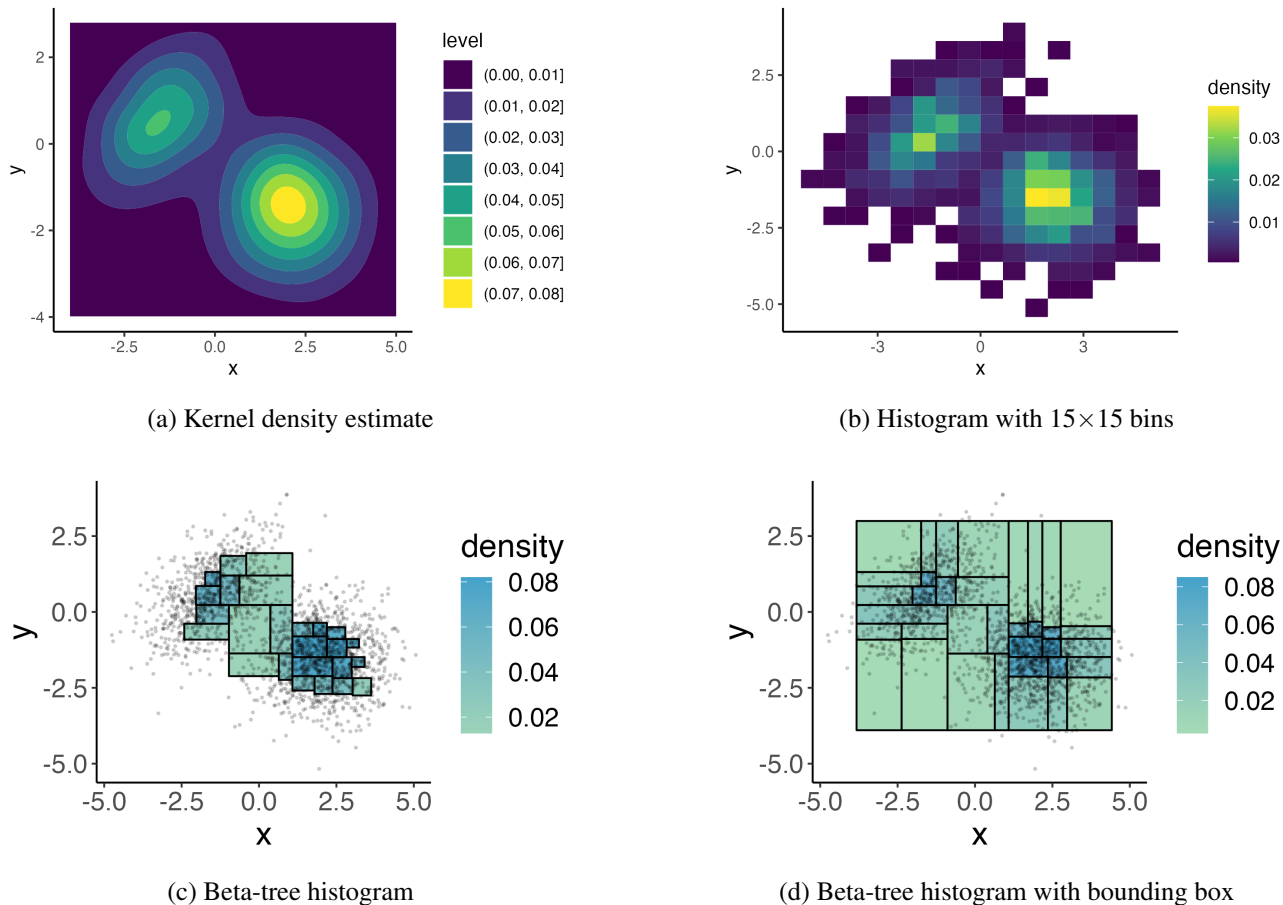


Figure 3: Density estimate and histograms for a mixture of two-dimensional Gaussians, $n = 2000$.

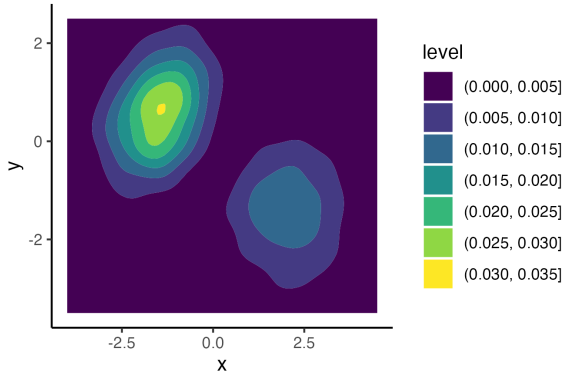
the plane $z = 1$ as well as observations that lie in a slab where $0.8 \leq z \leq 1.2$.

Second, we plot a histogram with a fixed number of 15 equally sized bins in each dimension, see Figures 3b and 4b. For the three-dimensional mixture the resulting histogram has $15^3 = 3375$ bins, of which only 834 are not empty.

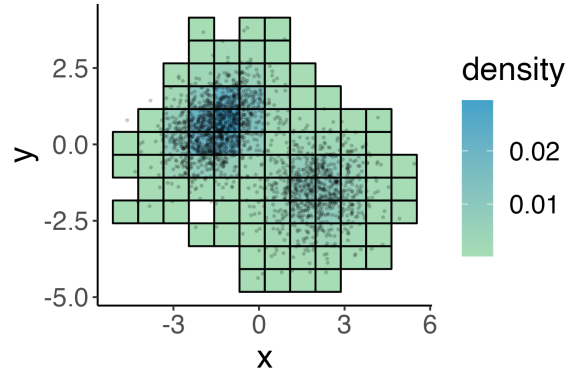
Third, we show the Beta-tree histogram with confidence level $1 - \alpha = 90\%$ in Figures 3c and 4c. The Beta-tree histogram consists of only 25 rectangles in the two-dimensional setting and 125 rectangles in the three-dimensional setting. This exemplifies how the Beta-tree histogram yields a more parsimonious summary of the data compared to a histogram with a fixed number of bins.

Figures 3d and 4d show the Beta-tree histogram with bounding box, which is obtained by excluding 0.5% of the data in each tail of each coordinate. The Beta-tree histogram with bounding box consists of 36 rectangles in the two-dimensional setting and 315 rectangles in the three-dimensional setting.

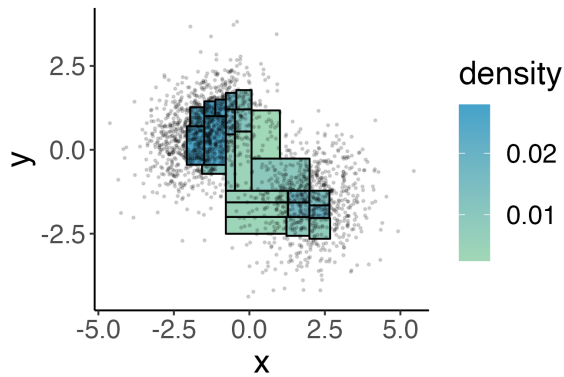
We note that Figure 4 suggests that all four methods are able to distinguish the first and the second components in the mixture. However, only the two Beta-tree methods provide a confidence statement to this effect. Section 5 gives more details for such multivariate mode hunting with finite sample guarantees.



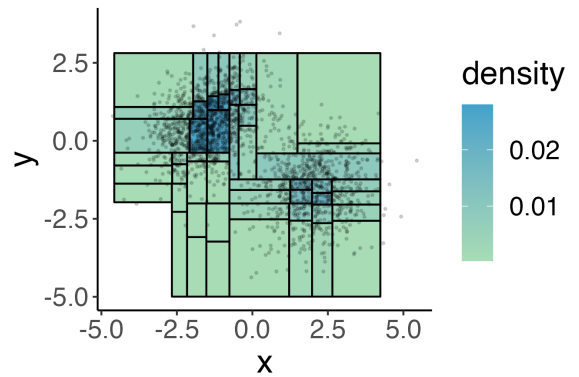
(a) Kernel density estimate



(b) Histogram with $15 \times 15 \times 15$ bins



(c) Beta-tree histogram



(d) Beta-tree histogram with bounding box

Figure 4: Density estimate and histograms for a mixture of three-dimensional Gaussians, $n = 20000$. The scatterplot shows all observations within a slab perpendicular to the z coordinate with $0.8 \leq z \leq 1.2$. We plot the histograms and kernel density estimates along a slice where $z = 1$, and we only show rectangles where the empirical density is at least 2×10^{-4} so that we do not plot empty rectangles.

5 Multivariate mode hunting

This section gives an example of how the Beta-tree can be used for inference, namely to perform multivariate mode detection with finite sample guarantees. The interest in multivariate mode hunting derives from the important problem of detecting subpopulations in a distribution. One prominent approach to this problem identifies such subpopulations with high density regions, see e.g. [22, 21, 44, 33, 18, 34, 9, 46]. This gives rise to the problem of finding confidence bounds for the number and location of modes in a density. Multivariate mode hunting is considered to be a difficult statistical problem due to the inherent multiple testing and due to the curse of dimensionality. Indeed, the statistical statements in the above references are typically of approximate or asymptotic nature.

Here we show how mode hunting can be performed by using the Beta-tree as a summary of the data. The advantage of using the Beta-tree for this task is that the analysis inherits the statistical guarantees that come with the Beta-tree.

In order to check that a density f has two separate modes at locations x and y , it is necessary to check that on every (possible curved) path that connects x and y , there is a point z with $f(z) < \min(f(x), f(y))$. This poses not only a statistical problem due to the simultaneous estimation of f , but also a computational problem since all paths would need to be checked. This has motivated various approximations proposed in the literature, such as checking only along convex combinations $z_\alpha = \alpha x + (1 - \alpha)y$, $0 \leq \alpha \leq 1$, see [9]. A Beta-tree makes it possible to avoid this restriction: Since the Beta-tree segments \mathbf{R}^d into rectangles for which we are confident that f is approximately constant, it is sufficient to check all paths of adjacent² rectangles in the Beta-tree. This is typically a manageable computational task since the number of rectangles in the Beta-tree is not large. For example, the group of rectangles in dark green in the top left and lower right corners in Figure 3c have higher density compared to the rectangles in between. Indeed, the underlying mixture distribution has two modes at $(1.5, 0.6)$ and $(2, -1.5)$. Moreover, the Beta-tree provides simultaneous confidence bounds (3) for the average density $f(R) = \int_R f(x)dx/|R|$ (which equals f on R if f is constant on R). This makes it straightforward to check the condition $f(R_1) < \min(f(R_2), f(R_3))$ by checking whether the upper confidence bound for $f(R_1)$ is smaller than the lower confidence bounds for $f(R_2)$ and $f(R_3)$. Since these confidence bounds are simultaneous, any statement involving such inequalities along multiple paths will inherit the finite sample confidence level $1 - \alpha$. In particular, it is possible to claim the existence of a certain number of modes with a finite sample guarantee.

We summarize our algorithm in Algorithm 1. In short, we first tag the rectangle with highest empirical density as a mode. Then, we iterate through the rectangles in the Beta-tree in descending order of their empirical density. For each rectangle R_i , we iterate through every path from R_i to every mode that has been tagged so far, and if we find a path where *no* rectangle along the path has lower density than both endpoints, then R_i will not be tagged as a mode.

We now apply our procedure to identify modes in the two mixture scenarios considered in Section 4. For faster computation we only considered paths with lengths at most 6. In the two-dimensional Gaussian mixture we identify two modes, whose corresponding rectangles are striped in Figure 5 (left). The true modes (shown as red asterisks) are close to these two rectangles. Figure 5 (right) shows the confidence intervals for the $f(R)$ along the shortest path (in terms of number of rectangles) between the two identified modes. The plot shows that there exists a rectangle whose upper confidence bound is below the minimum of the lower bounds for the two modal rectangles, which is marked by a dashed line.

For the three-dimensional mixture we are able to identify three modes. We report the locations of true modes

²Since $R_i = \times_{p=1}^d (l_{ip}, u_{ip})$, R_i and R_j are adjacent iff $[l_{ip}, u_{ip}] \cap [l_{jp}, u_{jp}] \neq \emptyset$ for all $p = 1, \dots, d$.

Algorithm 1: Multivariate mode hunting using the Beta-tree

Input: A Beta-tree with N rectangles R_i and their empirical density h_i given by (5) and the lower and upper confidence bounds $f_L(R_i)$ and $f_U(R_i)$ given by (3). The list of modes \mathcal{M} is empty.

- 1 Compute the adjacency matrix $A \in \mathbb{Z}^{N \times N}$ such that $A_{i,j} = 1$ iff R_i and R_j are adjacent;
- 2 Order the rectangles R_i such that $h_1 \geq h_2 \geq \dots \geq h_N$;
- 3 Tag the region with the highest density as a mode: $\mathcal{M} = \{R_1\}$;
- 4 **for** $i = 2, \dots, N$ **do**
- 5 **for** $m \in \mathcal{M}$ (i.e. iterate through the current modes in \mathcal{M}) **do**
- 6 **for** Every path connecting R_i and m **do**
- 7 **if** There is no rectangle R along the path such that $f_U(R) < \min(f_L(m), f_L(R_i))$ **then**
- 8 | R_i is not a mode. Break the two inner for-loops and move on to R_{i+1} , i.e. $i \leftarrow i + 1$
- 9 **end**
- 10 **end**
- 11 Add R_i as a mode: $\mathcal{M} = \mathcal{M} \cup \{R_i\}$
- 12 **end**

Output: The list of modes \mathcal{M}

and the centers of the modal rectangles identified by the algorithm in Table 1. The estimated modes are again close to the true modes.

Table 1: The coordinates of the centers of the modal rectangles identified by the algorithm (“Estimated modes”) and of the true modes.

Index	Estimated modes	True modes
1	(-2.7,-3.0,-2.4)	(-2.6, -3, -2)
2	(-1.0,0.8,1.7)	(-1.5, 0.6, 1)
3	(1.7,-1.6,0.3)	(2, -1.5, 0)

6 A real data example

We now apply our approach to visualize and identify cell populations in flow cytometry data. In [8], flow cytometry was used to analyze peripheral blood samples collected from patients who underwent a bone marrow transplant. The objective was to identify biomarkers which indicate graft-versus-host disease (GvHD), which occurs in allogeneic hematopoietic stem cell transplant recipients when donor-immune cells attack tissue of the recipient. Researchers initially identified 121 subpopulations from 6 biomarkers, among which they pinpointed the population identified as CD3+ CD4+ CD8b+ to have the highest correlation with the development of acute GvHD.

A subset of the data from this research is publicly available in RvHD in the R package `mclust`. The data contain 9083 observations from a patient with GvHD and 6809 observations from a control patient. The data includes four biomarkers CD4, CD8b, CD3, and CD8. Since the sample size is limited, we will construct a histogram using only the the first two variables CD4 and CD8b.

We constructed a Beta-tree histogram using the data of the patient who developed GvHD (who we refer to as the case patient) and Algorithm 1 identifies two modes, which indicates the presence of two cell populations, see Figure 6a. We report the centers of the two modal rectangles in the column “Center” in Table 2. If these two



Figure 5: Left: Beta-tree histogram of a two-dimensional Gaussian mixture with confidence level $1 - \alpha = 0.9$. The modal rectangles are indicated by stripes and the red stars mark the two modes of the mixture distribution. Right: The confidence intervals for $f(R)$ for every rectangle along the shortest path between the two modes. The points indicate the empirical density in each rectangle and the dashed line shows the minimum of the lower confidence bounds for the two modal rectangles.

populations are indicative of GvHD, then the empirical density in these regions from the control patient, which is given in the column “Density (control)”, should be lower compared to that of the case patient. In this example, the empirical density of the control patient is indeed well below the confidence intervals for the case patient in both regions, suggesting that these regions might be specific to GvHD.

Finally, we compute a bounded Beta-tree histogram for CD4, CD8b, CD3 and visualize one slice of the histogram along the axis $CD3 = 1.0$. We also plot observations within the slab $0.8 \leq CD3 \leq 1.2$. The Beta-tree histogram captures one cluster of observations characterized by high values of CD4, CD8b and CD3, see Figure 6b.

Table 2: Column “Center” shows the the coordinates of the center of the modal rectangles in the sample collected from the case patient. Column “CI (Case)” shows the confidence intervals for the average densities of these two modal regions. Column “Density (Control)” reports the empirical density of the data collected from the control patient.

Center	CI (Case)	Density (Control)
(-0.13,0.01)	(0.42, 0.74)	0.009
(1.87, 1.59)	(0.03, 0.06)	0.0012

7 Discussion

This paper introduces Beta-trees for summarizing multivariate data. The Beta-tree possesses several important-properties: It provides a compact summary of the data by partitioning the sample space into rectangles on which the distribution is close to uniform. The partition is adaptive to the data, which is key for avoiding the curse of dimensionality. The probability content of each rectangle in the partition has a sampling distribution that is known exactly and thus allows to set finite sample confidence bounds. A multiscale Bonferroni adjustment results in simultaneous confidence bounds whose widths do not depend on the dimension and match the optimal univariate widths, thus avoiding the curse the dimensionality. The simultaneous validity of the confidence intervals allows

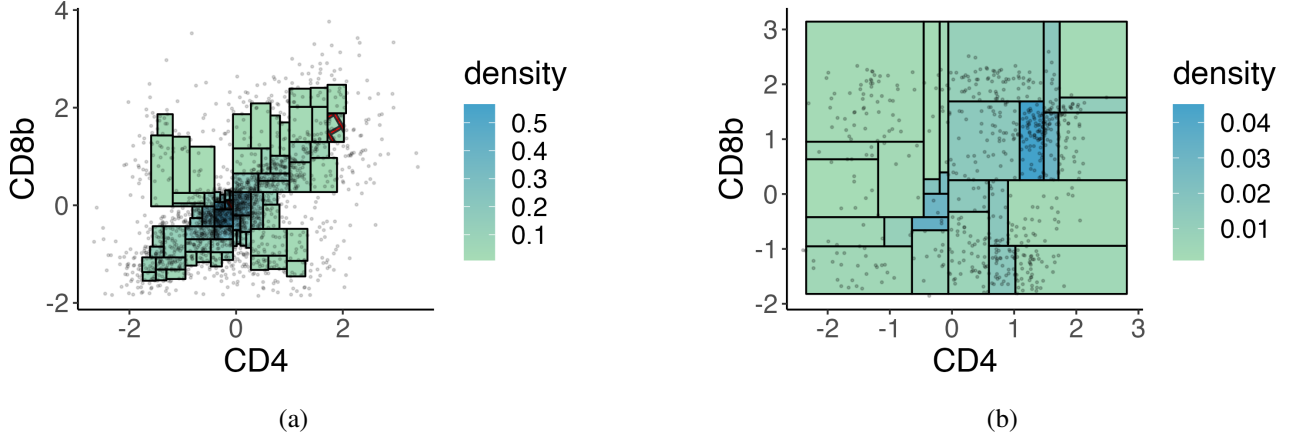


Figure 6: Beta-tree histograms of data from the case patient, $1 - \alpha = 0.9$. (a) A two-dimensional histogram of CD8b vs. CD4. The two identified modal rectangles are marked by red stripes. A random sample of 2000 observations is also shown. (b) A three-dimensional bounded Beta-tree histogram of CD4, CD8b, and CD3. The display shows rectangles in the Beta-tree histogram that intersect the plane $CD3 = 1.0$. The displayed points are observations within the slab $0.8 \leq CD3 \leq 1.2$.

to use Beta-trees for various data-analytic tasks. As an example, we showed how Beta-trees can be used for multivariate mode hunting with finite sample guarantees. We illustrated this with flow cytometry data.

8 Proofs

8.1 Proof of Proposition 1

The proof of Proposition 1 is based on the following result:

Proposition 2 *Let $X_1, \dots, X_n \in \mathbf{R}^d$ be i.i.d. with distribution F and let $g, h : \mathbf{R}^d \rightarrow \mathbf{R}$ be measurable functions. Write $g(X)_{(k)}$ for the k th order statistic of the $g(X_i)$, $i = 1, \dots, n$. For fixed j and k with $1 \leq j < k \leq n$ set*

$$\begin{aligned}
 R &:= \left\{ x \in \mathbf{R}^d : g(x) < g(X)_{(k)} \right\}, \\
 \{Y_1, \dots, Y_{k-1}\} &:= \{X_1, \dots, X_n\} \cap R, \\
 S &:= \left\{ x \in R : h(x) < h(Y)_{(j)} \right\}.
 \end{aligned}$$

Assume that F, g, h are such that the $g(X_i)$ and the $h(Y_i)$ have a continuous cdf, so R contains $\#R = k - 1$ observations a.s. and $\#S = j - 1$ a.s. Then

- (a) $F(R) \sim \text{Beta}(\#R + 1, n - \#R)$
- (b) $\frac{F(S)}{F(R)} \sim \text{Beta}(\#S + 1, \#R - \#S)$
- (c) $\frac{F(S)}{F(R)}$ and $F(R)$ are independent
- (d) $F(S) \sim \text{Beta}(\#S + 1, n - \#S)$

(e) The results (a)–(d) continue to hold when the above construction is iterated, starting with the above S in place of R and using prescribed functions g and h that may be different from the initial functions.

We point out that this result requires that k and j , and hence $\#R$ and $\#S$, are prescribed (i.e. do not depend on the data), and that the inequalities in the definition of R and S are strict as using ‘ \leq ’ for R will add one observation to R which will generally invalidate the beta distribution for $F(S)$.

The first such result about the beta distribution of $F(S)$ for multivariate S constructed from order statistics appears to be Wald (1943), who considered the special case where g and h are univariate marginals [49]. Wald’s proof has an important gap which was patched by Tukey (1947) with a lemma that he called ‘Wald’s Principle’ [48]. The works of Wald and Tukey are hampered by the methodology available in the 1940s. We provide a short and elementary proof of Proposition 2 and a more general version of Wald’s Principle in Lemma 1.

Lemma 1 (Wald’s Principle) *Let $X_1, \dots, X_n \in \mathbf{R}^d$ be i.i.d. with distribution F and let $g : \mathbf{R}^d \rightarrow \mathbf{R}$ be a measurable function. Suppose F and g are such that the univariate random variables $g(X_i)$ have a continuous cdf. Fix $k \in \{1, \dots, n\}$ and write $g(X)_{(k)}$ for the k th order statistic of the $g(X_i)$, $i = 1, \dots, n$. Then divide the X_i into two groups according to whether $g(X_i)$ is smaller or larger than $g(X)_{(k)}$:*

$$\begin{aligned} \{Y_1, \dots, Y_{k-1}\} &:= \{X_i : g(X_i) < g(X)_{(k)}\} \\ \{Z_1, \dots, Z_{n-k}\} &:= \{X_i : g(X_i) > g(X)_{(k)}\} \end{aligned}$$

where the Y_i and the Z_i are enumerated in the original order of outcome among the X_i .

Then, conditional on $g(X)_{(k)} = t$:

(a) The $\{Y_i\}$ and the $\{Z_i\}$ are independent.

(b) The Y_1, \dots, Y_{k-1} are i.i.d. with distribution $G(\cdot) = \frac{F(\cdot \cap R_t)}{F(R_t)}$ and the Z_1, \dots, Z_{n-k} are i.i.d. with distribution $K(\cdot) = \frac{F(\cdot \cap R_t^c)}{F(R_t^c)}$, where $R_t := \{x \in \mathbf{R}^d : g(x) < t\}$.

The lemma can be seen as a generalization of the following well known fact about univariate order statistics: Conditional on $X_{(k)} = t$, the vectors $(X_{(1)}, \dots, X_{(k-1)})$ and $(X_{(k+1)}, \dots, X_{(n)})$ are independent and the joint law of $(X_{(1)}, \dots, X_{(k-1)})$ is that of the order statistics of $k - 1$ i.i.d. random variables with distribution $\frac{F(\cdot \cap (-\infty, t))}{F((-\infty, t))}$, see Theorem 1.8.1 in [38]. Lemma 1 generalizes this result by establishing that the unordered X_i corresponding to $(X_{(1)}, \dots, X_{(k-1)})$ are i.i.d., and by generalizing this result to multivariate X_i ordered via g .

Proof of Lemma 1: We first note that $g(X_i)$ having a continuous cdf implies that $g(X_i) = g(X)_{(k)}$ for exactly one index i a.s., hence there are a.s. $k - 1$ observations Y_i and $n - k$ observations Z_i .

For Borel sets $B_i, \tilde{B}_i \in \mathbf{R}^d$:

$$\begin{aligned} &\mathbb{P}\left(Y_1 \in B_1, \dots, Y_{k-1} \in B_{k-1}, Z_1 \in \tilde{B}_1, \dots, Z_{n-k} \in \tilde{B}_{n-k} \mid g(X)_{(k)} \in [t, t + dt)\right) \\ &= \frac{\mathbb{P}\left(\mathcal{A} := \left\{Y_i \in B_i \cap R_t \text{ for } i = 1, \dots, k - 1, Z_j \in \tilde{B}_j \cap R_{t+dt}^c \text{ for } j = 1, \dots, n - k, g(X)_{(k)} \in [t, t + dt)\right\}\right)}{\mathbb{P}\left(g(X)_{(k)} \in [t, t + dt)\right)} \end{aligned} \tag{7}$$

We now write \mathcal{A} in terms of the X_i : Let $T_{k,n}$ be the set of permutations τ of $\{1, \dots, n\}$ such that $\tau(1) < \tau(2) < \dots < \tau(k-1)$ and $\tau(k+1) < \tau(k+2) < \dots < \tau(n)$. Since the Y_i and the Z_j are enumerated in the original order of outcome among the X_i we must have $Y_i = X_{\tau(i)}$ and $Z_j = X_{\tau(k+j)}$ for some $\tau \in T_{k,n}$. In fact, it is readily seen that $\mathcal{A} = \bigcup_{\tau \in T_{k,n}} B_\tau$, where

$$B_\tau := \left\{ X_{\tau(i)} \in B_i \cap R_t \text{ for } i = 1, \dots, k-1, X_{\tau(k+j)} \in \tilde{B}_j \cap R_{t+dt}^c \text{ for } j = 1, \dots, n-k, X_{\tau(k)} \in R_{t+dt} \setminus R_t \right\}.$$

The B_τ are mutually disjoint because different τ result in different assignments of the X_i to R_t , $R_{t+dt} \setminus R_t$ and R_{t+dt}^c . There are $\binom{n}{k-1}(n-k+1) = \frac{n!}{(k-1)!(n-k)!}$ permutations in $T_{k,n}$: there are $\binom{n}{k-1}$ ways to choose $\tau(1) < \dots < \tau(k-1)$ and $n-k+1$ possibilities for $\tau(k)$, which then uniquely determine $\tau(k+1) < \dots < \tau(n)$. Therefore

$$\mathbb{P}(\mathcal{A}) = \sum_{\tau \in T_{k,n}} \mathbb{P}(B_\tau) = \frac{n!}{(k-1)!(n-k)!} \left(\prod_{i=1}^{k-1} F(B_i \cap R_t) \right) \left(\prod_{j=1}^{n-k} F(\tilde{B}_j \cap R_{t+dt}^c) \right) dF_g(t) \quad (8)$$

where F_g denotes the cdf of $g(X_1)$ and $dF_g(t) = F_g(t+dt) - F_g(t)$. As for the denominator of (7), since F_g is continuous it is known that the univariate k th order statistic $g(X)_{(k)}$ has the following density w.r.t. the cdf F_g :

$$\mathbb{P}\left(g(X)_{(k)} \in [t, t+dt)\right) = \frac{n!}{(k-1)!(n-k)!} \left(F_g(t)\right)^{k-1} \left(1 - F_g(t)\right)^{n-k} dF_g(t),$$

see Theorem 1.5.1 in [38]. Using $F_g(t) = F(R_t)$ and (8) shows that (7) equals

$$\prod_{i=1}^{k-1} \frac{F(B_i \cap R_t)}{F(R_t)} \prod_{j=1}^{n-k} \frac{F(\tilde{B}_j \cap R_t^c)}{F(R_t^c)}$$

which establishes the claims of the lemma.

As an aside we note that it appears to be surprisingly difficult to establish this result via conditional distributions rather than by calculating probabilities of $[t, t+dt)$. In the univariate setting, Theorem 1.8.1 in [38] shows that conditional on $X_{(k)}$, the order statistics to the left of $X_{(k)}$ are independent of those to the right, and the proof of Corollary 1.8.4 and problem 1.33 can be used to extend this result to the unordered observations as in claim (a) of the Lemma. Already in that univariate setting these proofs with conditional distributions are rather complicated. \square

Proof of Proposition 2: We will use the following two well known facts:

Fact 1 *If the univariate Z_1, \dots, Z_n are i.i.d. with a continuous cdf G , then $G(Z_{(k)}) \sim \text{Beta}(k, n+1-k)$.*

Fact 2 *If $V \sim \text{Beta}(\alpha, \beta)$ and $W \sim \text{Beta}(\alpha + \beta, \gamma)$ are independent, the $VW \sim \text{Beta}(\alpha, \beta + \gamma)$.*

Write F_g for the univariate cdf of $g(X_1)$. Then $F(R) = F_g(g(X)_{(k)}) \sim \text{Beta}(k, n+1-k)$ by Fact 1, proving (a).

By Lemma 1, conditional on $g(X)_{(k)}$ the Y_1, \dots, Y_{k-1} are i.i.d. with distribution $G(\cdot) = \frac{F(\cdot \cap R)}{F(R)}$. Write G_h

for the cdf of $h(Y_1)$, so for real t :

$$G_h(t) = G(\{x \in \mathbf{R}^d : h(x) \leq t\}) = \frac{F(\{x \in \mathbf{R}^d : h(x) \leq t\} \cap R)}{F(R)}.$$

By the definition of S :

$$\frac{F(S)}{F(R)} = G_h(h(Y)_{(j)}) \sim \text{Beta}(j, k - j)$$

by Fact 1. Since this conditional distribution given $g(X)_{(k)}$, i.e. given R , does not depend on R as $\#R = k - 1$ is fixed, it follows that this result also holds unconditionally and that $\frac{F(S)}{F(R)}$ and $F(R)$ are independent, proving (b) and (c).

(d) follows from Fact 2 and (a)–(c): set $\alpha := j$, $\beta := k - j$, $\gamma := n + 1 - k$ in Fact 2.

As for (e), the above proof goes through if one iterates this construction starting with S in place of R . In particular, applying Lemma 1 again to the conditional distribution given R , $G(\cdot) = \frac{F(\cdot \cap R)}{F(R)}$, shows that the conditional distribution given S is

$$\frac{\frac{F(\cdot \cap R \cap S)}{F(R)}}{\frac{F(S \cap R)}{F(R)}} = \frac{F(\cdot \cap S)}{F(S)} \quad \text{since } S \subset R. \quad \square$$

Proof of Proposition 1: This follows from Proposition 2 by taking g, h to be functions of the form $x \mapsto \pm x_p$ for $p \in \{1, \dots, d\}$, i.e. by selecting a certain univariate marginal and choosing the sign of x_p to select the observations to the left or to the right of the order statistic of that marginal. Note that F being continuous implies that these $g(X_i)$ and $h(Y_i)$ have a continuous cdf. This proposition also applies to selecting observations inside a bounding box if that box is constructed as described in Section 2.1. \square

8.2 Proof of Theorem 1

Consider R_k at tree level D and write $p_D := \frac{n_k+1}{n+1}$. Then Proposition 1 gives $F(R_k) \sim \text{Beta}((n+1)p_D, (n+1)(1-p_D))$. Let $x_{up} := q\text{Beta}(1 - \frac{\alpha_D}{2}, (n+1)p_D, (n+1)(1-p_D))$ be the upper confidence bound of $C_k(\alpha_D)$. Then

$$\frac{\alpha_D}{2} = \mathbb{P}(F(R_k) \geq x_{up}) \leq \exp(-(n+1)\Psi(x_{up}, p_D))$$

by Proposition 2.1 in [15], where $\Psi(x, p) := p \log \frac{p}{x} + (1-p) \log \frac{1-p}{1-x}$. Hence $\Psi(x_{up}, p_D) \leq \frac{1}{n+1} \log \frac{2}{\alpha_D}$. Using the inequality at the end of said proposition, this implies

$$x_{up} - p_D \leq \sqrt{2p_D(1-p_D) \frac{\log \frac{2}{\alpha_D}}{n+1}} + (1-2p_D)^+ \frac{\log \frac{2}{\alpha_D}}{n+1}$$

In the same way one finds an (even tighter) inequality for the lower confidence bound x_{low} of $C_k(\alpha_D)$:

$$x_{low} - p_D \geq -\sqrt{2p_D(1-p_D) \frac{\log \frac{2}{\alpha_D}}{n+1}}$$

Therefore

$$\sup_{x \in C_k(\alpha_D)} \sqrt{n} \frac{|x - p_D|}{\sqrt{p_D(1-p_D)}} \leq \sqrt{2 \log \frac{2}{\alpha_D}} + \frac{\log \frac{2}{\alpha_D}}{\sqrt{np_D(1-p_D)}} \quad (9)$$

Using $2^D \sim \frac{1}{p_D}$, $D_{max} \sim \log_2 n$ and $\sum_{B=2}^{D_{max}} \frac{1}{B} \sim \log \log_2 n$, we obtain $\frac{2}{\alpha_D} \leq 2^{\frac{(\log_2 n)(\log \log_2 n)}{\alpha p_D}}$, hence

$$\log \frac{2}{\alpha_D} \leq (1 + \epsilon_n) \log \frac{e}{p_D}, \quad \text{with } \epsilon_n := \frac{\log \left(\frac{2}{\alpha} (\log_2 n) (\log \log_2 n) \right)}{\log n^{1-q}}$$

since $p_D \leq n^{q-1}$. Furthermore, $p_D \geq \frac{\log^2 n}{n}$ yields

$$\frac{\log \frac{2}{\alpha}}{\sqrt{np_D(1-p_D)}} \leq \frac{\frac{3}{2} \log \frac{e}{p_D}}{\log n} \leq \frac{3}{2} \sqrt{\frac{\log \frac{e}{p_D}}{\log n}}$$

This allows to bound (9) as follows:

$$\begin{aligned} \sup_{x \in C_k(\alpha_D)} \sqrt{n} \frac{|x - p_D|}{\sqrt{p_D(1-p_D)}} &\leq \sqrt{2(1 + \epsilon_n) \log \frac{e}{p_D}} + \frac{3}{2} \sqrt{\frac{\log \frac{e}{p_D}}{\log n}} \\ &\leq \left(\sqrt{2} + \epsilon_n + \frac{3}{2} \sqrt{\frac{1}{\log n}} \right) \sqrt{\log \frac{e}{p_D}} \end{aligned} \quad (10)$$

This essentially establishes the claim apart from having p_D in place of x in the denominator. However, (10) yields $\sup_{x \in C_k(\alpha_D)} |x - p_D| \leq \sqrt{\frac{p_D}{n}} \sqrt{3 \log \frac{e}{p_D}}$, so

$$\sup_{x \in C_k(\alpha_D)} \left| \frac{x}{p_D} - 1 \right| \leq \sqrt{\frac{3 \log \frac{e}{p_D}}{np_D}} \leq \sqrt{\frac{3}{\log n}}$$

which gives $\sup_{x \in C_k(\alpha_D)} \sqrt{\frac{p_D(1-p_D)}{x(1-x)}} \leq 1 + \sqrt{\frac{3}{\log n}}$. Therefore

$$\begin{aligned} \sup_{x \in C_k(\alpha_D)} \sqrt{n} \frac{|x - p_D|}{\sqrt{x(1-x)}} &\leq \left(\sqrt{2} + \epsilon_n + \frac{3}{2\sqrt{\log n}} \right) \left(1 + \sqrt{\frac{3}{\log n}} \right) \sqrt{\log \frac{e}{p_D}} \\ &\leq \left(\sqrt{2} + \frac{4}{\sqrt{\log n}} \right) \sqrt{\log \frac{e}{p_D}} \end{aligned}$$

for n large enough. \square

References

- [1] J. Acharya, I. Diakonikolas, C. Hegde, J. Li, and L. Schmidt. Fast and near-optimal algorithms for approximating distributions by histograms. In *Proceedings of the 34th ACM SIGMOD-SIGACT-SIGAI Symposium on Principles of Database Systems*, pages 249–263, 2015.
- [2] J. Acharya, I. Diakonikolas, J. Li, and L. Schmidt. Sample-optimal density estimation in nearly-linear time. In *Proceedings of the Twenty-Eighth Annual ACM-SIAM Symposium on Discrete Algorithms*, pages

1278–1289, 2017.

- [3] N. Aghaeepour, G. Finak, H. Hoos, T. R. Mosmann, R. Brinkman, R. Gottardo, R. H. Scheuermann, T. F. Consortium, and T. D. Consortium. Critical assessment of automated flow cytometry data analysis techniques. *Nature Methods*, 10(3):228–238, 2013.
- [4] R. E. Bellman. *Adaptive control processes*. Princeton University Press, Princeton, NJ, 1961.
- [5] J. L. Bentley. Multidimensional binary search trees used for associative searching. *Commun. ACM*, 18(9):509–517, 1975.
- [6] L. Birgé and Y. Rozenholc. How many bins should be put in a regular histogram. *ESAIM: Probability and Statistics*, 10:24–45, 1 2006. electronic.
- [7] R. R. Brinkman, N. Aghaeepour, G. Finak, R. Gottardo, T. Mosmann, and R. H. Scheuermann. Automated analysis of flow cytometry data comes of age. *Cytometry Part A*, 89(1):13–15, 2016.
- [8] R. R. Brinkman, M. Gasparetto, S.-J. J. Lee, A. J. Ribickas, J. Perkins, W. Janssen, R. Smiley, and C. Smith. High-content flow cytometry and temporal data analysis for defining a cellular signature of graft-versus-host disease. *Biol. Blood Marrow Transplant.*, 13(6):691–700, 2007.
- [9] P. Burman and W. Polonik. Multivariate mode hunting: Data analytic tools with measures of significance. *J. Multivar. Anal.*, 100(6):1198–1218, 2009.
- [10] J. E. Chacón and T. Duong. Multivariate plug-in bandwidth selection with unconstrained pilot bandwidth matrices. *TEST*, 19(2):375–398, 2010.
- [11] S. Chan, I. Diakonikolas, R. Servedio, and X. Sun. Near-optimal density estimation in near-linear time using variable-width histograms. In *Advances in Neural Information Processing Systems*, pages 1844–1852, 2014.
- [12] P. Chattopadhyay, T. Gierahn, M. Roederer, and J. Love. Single-cell technologies for monitoring immune systems. *Nature Immunology*, 15:128–135, 2014.
- [13] I. Diakonikolas, D. Kane, and J. Peebles. Testing identity of multidimensional histograms. In *Proceedings of Machine Learning Research*, volume 99, pages 1–25, 2019.
- [14] I. Diakonikolas, J. Li, and L. Schmidt. Fast and sample near-optimal algorithms for learning multidimensional histograms. In *Proceedings of the 31st Conference On Learning Theory*, volume 75, pages 819–842, 2018.
- [15] L. Dümbgen. New goodness-of-fit tests and their application to nonparametric confidence sets. *The Annals of Statistics*, 26(1):288 – 314, 1998.
- [16] D. Freedman and P. Diaconis. On the histogram as a density estimator: L2 theory. *Zeitschrift für Wahrscheinlichkeitstheorie und Verwandte Gebiete*, 57(4):453–476, 1981.
- [17] D. Freedman, R. Pisani, and R. Purves. *Statistics*. W.W.Norton, New York, 4th edition, 2007.
- [18] J. Friedman and N. Fisher. Bump hunting in high-dimensional data. *Comput. Statist.*, 9:123–143, 1999.

- [19] J. H. Friedman, J. L. Bentley, and R. A. Finkel. An algorithm for finding best matches in logarithmic expected time. *ACM Trans. Math. Softw.*, 3(3):209–226, 1977.
- [20] A. Gilbert, S. Guha, P. Indyk, Y. Kotidis, S. Muthukrishnan, and M. Strauss. Fast, small-space algorithms for approximate histogram maintenance. In *Proceedings of the thirty-fourth annual ACM symposium on Theory of computing*, pages 389–398, 2002.
- [21] I. Good and R. Gaskins. Density estimation and bump hunting by the penalized maximum likelihood method exemplified by scattering and meteorite data. *J. Amer. Statist. Assoc.*, 75:42–73, 1980.
- [22] J. Hartigan. *Clustering Algorithms*. Wiley, New York, 1975.
- [23] P. Indyk, R. Levi, and R. Rubinfeld. Approximating and testing k-histogram distributions in sub-linear time. In *Proceedings of the 31st ACM SIGMOD-SIGACT-SIGAI symposium on Principles of Database Systems*, pages 15–22, 2012.
- [24] H. Jagadish, N. Koudas, S. Muthukrishnan, V. Poosala, K. Sevcik, and T. Suel. Optimal histograms with quality guarantees. In *Proceedings of the International Conference on Very Large Data Bases*, pages 275–286, 2014.
- [25] J. Klemelä. Multivariate histograms with data-dependent partitions. *Statist. Sinica*, 19(1):159–176, 2009.
- [26] D. Li, K. Yang, and W. H. Wong. Density estimation via discrepancy based adaptive sequential partition. *Adv Neural Inf Process Syst.*, 29:1091–1099, 2016.
- [27] H. Li, A. Munk, H. Sieling, and G. Walther. The essential histogram. *Biometrika*, 107(2):347–364, 2020.
- [28] L. Liu and W. H. Wong. Multivariate density estimation via adaptive partitioning (i): Sieve mle, 2014.
- [29] L. Liu and W. H. Wong. Multivariate density estimation via adaptive partitioning (ii): Posterior concentration, 2015.
- [30] L. Lu, H. Jiang, and W. H. Wong. Multivariate density estimation by bayesian sequential partitioning. *J. Amer. Statist. Assoc.*, 108(504):1402–1410, 2013.
- [31] E. Lugli, M. Roederer, and A. Cossarizza. Data analysis in flow cytometry: the future just started. *Cytometry Part A*, 77:705 – 713, 2010.
- [32] K. M. McKinnon. Flow cytometry: An overview. *Curr. Protoc. Immunol.*, 120(1):5.1.1–5.1.11, 2018.
- [33] M. Minotte. Nonparametric testing of the existence of modes. *Ann. Statist.*, 25:1646–1660, 1997.
- [34] H. Ooi. Density visualization and mode hunting using trees. *J. Comput. Graph. Statist.*, 11(2):328–347, 2002.
- [35] B. Pollack, S. Bhattacharya, and M. Schmitt. Bayesian blocks in high energy physics: Better binning made easy!, 2017.
- [36] A. Rahim, J. Meskas, S. Drissler, A. Yue, A. Lorenc, A. Laing, N. Saran, J. White, L. Abeler-Dörner, A. Hayday, and R. R. Brinkman. High throughput automated analysis of big flow cytometry data. *Methods*, 134-135:164–176, 2018. Advanced Flow Cytometry Techniques for Clinical Detection.

- [37] P. Ram and A. G. Gray. Density estimation trees. In *Proceedings of the 17th ACM SIGKDD International Conference on Knowledge Discovery and Data Mining*, KDD '11, pages 627—635, New York, NY, USA, 2011. Association for Computing Machinery.
- [38] R. Reiss. *Approximate Distributions of Order Statistics: With Applications to Nonparametric Statistics*. Springer Series in Statistics. Springer-Verlag, New York, 1989.
- [39] S. R. Sain, K. A. Baggerly, and D. W. Scott. Cross-validation of multivariate densities. *J. Amer. Statist. Assoc.*, 89(427):807–817, 1994.
- [40] J. Scargle, J. Norris, B. Jackson, and J. Chiang. Studies in astronomical time series analysis VI. Bayesian block representations. *The Astrophysical Journal*, 764(2), 2013.
- [41] D. W. Scott. *Multivariate Density Estimation*. John Wiley & Sons, 2015.
- [42] S. J. Sheather and M. C. Jones. A reliable data-based bandwidth selection method for kernel density estimation. *J. R. Stat. Soc. Ser. B Methodol.*, 53(3):683–690, 1991.
- [43] G. Shorack and J. Wellner. *Empirical Processes with Applications to Statistics*. Wiley series in probability and mathematical statistics. Probability and mathematical statistics. Wiley, New York, 1986.
- [44] B. Silverman. Using kernel density estimates to investigate multimodality. *J. Roy. Statist. Soc. Ser. B*, 43:97–99, 1981.
- [45] C. J. Stone. Optimal Rates of Convergence for Nonparametric Estimators. *The Annals of Statistics*, 8(6):1348 – 1360, 1980.
- [46] W. Stuetzle and R. Nugent. A generalized single linkage method for estimating the cluster tree of a density. *J. Comput. Graph. Statist.*, 19:397–418, 2010.
- [47] N. Thaper, S. Guha, P. Indyk, and N. Koudas. Dynamic multidimensional histograms. In *Proceedings of the 2002 ACM SIGMOD international conference on Management of data*, pages 428–439, 2002.
- [48] J. W. Tukey. Non-parametric estimation ii. statistically equivalent blocks and tolerance regions—the continuous case. *Ann. Math. Stat.*, 18(4):529 – 539, 1947.
- [49] A. Wald. An extension of Wilks' method for setting tolerance limits. *Ann. Math. Stat.*, 14(1):45 – 55, 1943.
- [50] G. Walther and A. Perry. Calibrating the scan statistic: Finite sample performance versus asymptotics. *J. R. Stat. Soc. Ser. B Methodol.*, 84:1608–1639, 2022.
- [51] G. Walther, N. Zimmerman, W. Moore, D. Parks, and S. Meehan. Automatic clustering of flow cytometry data with density-based merging. *Advances in Bioinformatics*, 2009.
- [52] M. P. Wand and J. M. C. Multivariate plug-in bandwidth selection. *Comput. Stat.*, (9):97–116, 1994.

A More details about k -d trees and Beta-trees

This section gives some technical details about k -d trees that are relevant for implementing Beta-trees as a data structure.

The indexing R_k given in Section 2.1 is helpful if one wants to use algorithms that are not recursive. The standard definition of a k -d trees identifies a node with a splitting hyperplane. For implementing and working with a Beta-tree it is helpful to let a node represent a rectangle R_k and then add the following information to each node: The specification of R_k in terms of two bounds (which may be infinite) for each coordinate, the tree depth of the node (with the root node R_0 having depth 0), whether R_k is a leaf or not, the number n_k of data in the interior of R_k , lower and upper confidence bounds for $f(R_k)$ given in (3) and (4), and the pointers to the two children nodes.

For example, if the root node represents $R_0 = \mathbf{R}^d$, then R_0 contains all the data, so $n_0 = n$. The children have depth 1 and $n_1 = \lceil \frac{n_0}{2} \rceil - 1$, $n_2 = n_0 - \lceil \frac{n_0}{2} \rceil$. More generally, one obtains for $k \geq 0$: $n_{2k+1} = \lceil \frac{n_k}{2} \rceil - 1$, $n_{2k+2} = n_k - \lceil \frac{n_k}{2} \rceil$. If one uses a bounding box as described in Section 2.1, then R_0 is the bounding box and n_0 is the number of observations in the bounding box rather than n .

At tree depth $D \geq 0$ the k -d tree partitions R_0 into 2^D rectangles if all rectangles are split (which may not be the case for larger D due to the stopping criterion and the fact that the rectangles at a given depth don't contain exactly the same number of observations.) If R_0 is a bounding box, then all of these rectangles are bounded, hence $N_D = 2^D$ if all rectangles are split, whereas if $R_0 = \mathbf{R}^d$ and if all rectangles are split, then the number of bounded rectangles can be shown to be $N_D = \prod_{i=1}^d \left(2^{\lceil \frac{D+1-i}{d} \rceil} - 2 \right)_+$, which is zero for $D < 2d$ but nonzero for $D \geq 2d$. Therefore in the case $R_0 = \mathbf{R}^d$ the weighted Bonferroni adjustment (2) needs to be modified as follows:

$$\alpha_D = \frac{\alpha}{N_D(D_{max} - D + 2) \sum_{B=2}^{D_{max}-2d+2} \frac{1}{B}}, \quad D \geq 2d,$$

and $\alpha_D = 0$ for $D < 2d$. N_D can be easily found by traversing the k -d tree. This is preferable to the formulas for N_D given above since those hold only as long as all rectangles at a given depth are split.

Assuming all n observations are distinct in each of the d coordinates (which is the case with probability 1 if the distribution F is continuous), then each splitting hyperplane contains exactly one observation X_i . Therefore at tree depth D there are 2^D rectangles R_k and $2^D - 1$ observations X_i that don't belong to any of those R_k since they lie on the boundary of some R_k . This motivates to define the empirical measure as $F_n(R_k) = \frac{n_k+1}{n}$ rather than $F_n(R_k) = \frac{n_k}{n}$. This convention also turns out to be convenient for formulating the technical results in the paper.

Finding the maximal rectangles that are bounded and satisfy the goodness-of-fit (GOF) condition:

Due to the tree structure, this can be done recursively as follows:

Starting with the rectangle R being the root node: If R is bounded and satisfies the GOF condition $\widetilde{\text{lower}}(R) \leq h \leq \widetilde{\text{upper}}(R)$, then R is a maximal rectangle. Else if R is not a leaf, then call this procedure for the first child of R in place of R , then for the second child of R in place of R .

Alternatively, an iterative algorithm proceeds as follows:

for tree depths $D = 0, \dots, D_{max}$:

for rectangles R at tree depth D :

if (R is bounded and satisfies the GOF condition) **then** (R is maximal; delete the subtree below R)